



LAWRENCE  
LIVERMORE  
NATIONAL  
LABORATORY

# $^{235}\text{U}$ - $^{231}\text{Pa}$ age dating of uranium-rich materials for nuclear forensic investigations

G. R. Eppich, R. W. Williams, A. M. Gaffney, K. C. Schorzman

February 5, 2013

Journal of Analytical Atomic Spectrometry

## **Disclaimer**

---

This document was prepared as an account of work sponsored by an agency of the United States government. Neither the United States government nor Lawrence Livermore National Security, LLC, nor any of their employees makes any warranty, expressed or implied, or assumes any legal liability or responsibility for the accuracy, completeness, or usefulness of any information, apparatus, product, or process disclosed, or represents that its use would not infringe privately owned rights. Reference herein to any specific commercial product, process, or service by trade name, trademark, manufacturer, or otherwise does not necessarily constitute or imply its endorsement, recommendation, or favoring by the United States government or Lawrence Livermore National Security, LLC. The views and opinions of authors expressed herein do not necessarily state or reflect those of the United States government or Lawrence Livermore National Security, LLC, and shall not be used for advertising or product endorsement purposes.

Eppich GR; Williams RW; Gaffney AM; Schorzman KC.

$^{235}\text{U}$ - $^{231}\text{Pa}$  age dating of uranium-rich materials for nuclear forensic investigations

## ABSTRACT

Age dating of nuclear material can provide insight into source and suspected use in nuclear forensic investigations. We report here a method for the determination of the date of most recent chemical purification for uranium-rich materials using the  $^{235}\text{U}$ - $^{231}\text{Pa}$  chronometer. Protactinium is separated from uranium and neptunium matrices using anion exchange resin, followed by sorption of Pa to an  $\text{SiO}_2$  medium. The concentration of  $^{231}\text{Pa}$  is measured by isotope dilution mass spectrometry using  $^{233}\text{Pa}$  spikes prepared from an aliquot of  $^{237}\text{Np}$  and calibrated in-house using the rock standard Table Mountain Latite and the uranium isotopic standard U100. Combined uncertainties of age dates using this method are  $\sim 1.5$  to  $3.5\%$ , an improvement over alpha spectrometry measurement methods. Model ages of five uranium standard reference materials are presented; all standards have concordant  $^{235}\text{U}$ - $^{231}\text{Pa}$  and  $^{234}\text{U}$ - $^{230}\text{Th}$  model ages.

## INTRODUCTION

The illicit trafficking of uranium-rich materials presents a significant threat to the safety and security of the world. Nuclear forensic analyses, alongside conventional forensics, can provide valuable insight into the source, destination, and suspected use of interdicted nuclear materials. In this context, the age of a uranium-rich sample, defined as the time since the most recent chemical purification, is a useful

descriptive parameter of the material that does not require comparison against a database. The  $^{235}\text{U}$ - $^{231}\text{Pa}$  chronometer, commonly used in geochemistry (*e.g.*, Pickett *et al.*, 1994; Cheng *et al.*, 1998), is particularly amenable to age determination of uranium-rich materials due to the high uranium concentration and, in some cases, the  $^{235}\text{U}$ -enriched isotopic composition. It must be kept in mind that the “age” is really a “model-age,” because it depends on the model assumptions, first, of closed-system behavior (no loss of  $^{231}\text{Pa}$ , or gain other than from decay of  $^{235}\text{U}$ ), and second, that the initial concentration of  $^{231}\text{Pa}$  at the time of U purification was zero. However, in this paper, we dispense with the prefix “model” when using the terms “age” and “date,” but it is implicit. The  $^{235}\text{U}$ - $^{231}\text{Pa}$  chronometer can be used in concert with the  $^{234}\text{U}$ - $^{230}\text{Th}$  chronometer (*e.g.*, LaMont and Hall, 2005; Varga and Surányi, 2007; Williams and Gaffney, 2011) to assess the accuracy of the age. In the case of concordant ages using two different chronometers, confidence in that age as the purification date of U is strengthened. If the ages are discordant, one, or both, may be inaccurate, or the sample may have experienced a complex, multi-stage purification process affecting the daughter isotopes differently. Although in this case, the younger age represents the maximum possible age of the material, a useful datum in a nuclear forensic study.

In this paper, we present the first open-literature mass spectrometry study of the  $^{235}\text{U}$ - $^{231}\text{Pa}$  chronometer for nuclear forensic investigations. Uranium-rich materials were analyzed for  $^{235}\text{U}$  and  $^{231}\text{Pa}$  concentrations by multi-collector inductively coupled plasma mass spectrometry (MC-ICPMS). Dates for a suite of certified

reference materials distributed by New Brunswick Laboratory (NBL CRMs, uranium isotopic composition varying from depleted to highly-enriched) are presented.

Chemical separation techniques are presented that have been optimized for uranium-rich materials, resulting in simplified procedures and improved Pa recovery. Calibration of the  $^{233}\text{Pa}$  tracer, using both the rock-standard Table Mountain Latite (TML) (Williams *et al.*, 1992; and Sims *et al.*, 2008) and NBL CRM U100, is described, as are the age calculations, including a thorough treatment of uncertainty.

Dates using the  $^{235}\text{U}$ - $^{231}\text{Pa}$  chronometer show excellent agreement with  $^{234}\text{U}$ - $^{230}\text{Th}$  dates (Williams and Gaffney, 2011) for all of the NBL CRMs analyzed in this study. Expanded uncertainties on  $^{235}\text{U}$ - $^{231}\text{Pa}$  ages are 1.5-3.5 %, an improvement over the 3.5-5 % uncertainties reported by alpha spectrometry for the  $^{235}\text{U}$ - $^{231}\text{Pa}$  chronometer (Morgenstern *et al.*, 2002). In all but one case (NBL CRM U100), dates are older than reported production dates, suggesting incomplete purification of U from the daughters  $^{230}\text{Th}$  and  $^{231}\text{Pa}$ .

## METHODS

### *Production and calibration of the $^{233}\text{Pa}$ spike*

Determination of the  $^{235}\text{U}$ - $^{231}\text{Pa}$  age depends on precise and accurate measurement of  $^{235}\text{U}$  and  $^{231}\text{Pa}$  concentration. Measurement of  $^{235}\text{U}$  concentration by isotope dilution mass spectrometry (IDMS) is a routine procedure in geochemistry and

nuclear forensics, and is described elsewhere (*e.g.*, Williams and Gaffney, 2011). Measurement of  $^{231}\text{Pa}$  concentration can also be performed by IDMS with  $^{233}\text{Pa}$  as the spike isotope. Due to the short half-life of  $^{233}\text{Pa}$  ( $26.967 \pm 0.004$  days; Jones *et al.*, 1986), no certified  $^{233}\text{Pa}$  spike exists. Rather, the spike must be prepared immediately prior to use and calibrated for  $^{233}\text{Pa}$  concentration (atoms of  $^{233}\text{Pa}/\text{g}$ ) for its working-lifetime of approximately 3-4 months.

In this study,  $^{233}\text{Pa}$  spikes were prepared from a  $^{237}\text{Np}$  ( $t_{1/2} = 2.14$  My, alpha decay to  $^{233}\text{Pa}$ ) starting material. Approximately 20 mg of  $^{237}\text{Np}$  with  $^{233}\text{Pa}$  in secular equilibrium was dissolved in 9 M HCl + 0.05 M HF in a Teflon vial with 0.1 mL of concentrated  $\text{HClO}_4$ . The Np was dried and re-dissolved in  $\sim 6$  mL of 9 M HCl + 25  $\mu\text{L}$  saturated  $\text{H}_3\text{BO}_3$  + 50  $\mu\text{L}$  concentrated  $\text{HNO}_3$ . A Poly-Prep column (Bio-Rad) was loaded with 4 mL AG-1 X8 (100-200 mesh) anion exchange resin (Bio-Rad) and conditioned with  $>12$  mL 9 M HCl. The Np solution was loaded on the column and the vial was rinsed twice with 1 mL 9 M HCl, and the rinses were loaded onto the column. The column was then washed with 4 mL 9 M HCl. Some Np (as  $\text{Np(V)}$ ) is not sorbed on the resin and is recovered in the load and rinses. At this point, sorbed Np was clearly visible as a dark band in the top 1-2 mL of the resin bed. A new Teflon vial was then placed underneath the column to collect the Pa fraction and Pa was eluted with 12 mL 9 M HCl + 0.01 M HF (added in 2 mL increments).

Throughout this procedure, care was taken to avoid disturbing the resin, ensuring that sorbed Np remained in the upper 2 mL of the resin bed. Several drops of concentrated  $\text{HClO}_4$  were added to the vial containing the Pa, and the solution was

dried. A Teflon vial was then positioned underneath the column to recover Np, which was eluted with 30-60 mL 1 M HCl + 0.5 M HF, combined with the load and rinse fraction, dried and stored for future milkings of  $^{233}\text{Pa}$ . The Pa fraction was re-dissolved in 9 M HCl + 25  $\mu\text{L}$  of saturated  $\text{H}_3\text{BO}_3$  + 50  $\mu\text{L}$  of concentrated  $\text{HNO}_3$ , and the anion exchange separation technique was repeated using a smaller column volume ( $\sim 2$  mL) and proportionally smaller load, wash, and elution volumes.

Following the two previous anion exchange separation steps, the Pa fraction was dried and re-dissolved in 2 %  $\text{HNO}_3$  (by volume) + 25  $\mu\text{L}$  of saturated  $\text{H}_3\text{BO}_3$ . The next purification steps take advantage of the well-known behavior of Pa to sorb to  $\text{SiO}_2$  media. Quartz wool serves as the separation medium and is packed in a Poly-Prep column to a volume of approximately 2 mL and conditioned with  $>6$  mL of 2 %  $\text{HNO}_3$ . The hydrolyzed species  $\text{Pa}(\text{OH})_5$  readily sorbs to the wool, and other elements such as Np and U wash through. Pa is recovered by adding trace HF to the elution solution. The Pa solution was loaded onto the column. The vial was rinsed with 3 mL of 2 %  $\text{HNO}_3$ , and the rinses were added to the column. The column was washed with 4 mL 2 %  $\text{HNO}_3$ . A new Teflon vial was then placed under the column to collect Pa which was eluted with 6 mL 2 %  $\text{HNO}_3$  + 0.05 M HF, added in increments of 2 mL. Several drops of concentrated  $\text{HClO}_4$  were added to the vial containing Pa, and it was dried and re-dissolved in 2 %  $\text{HNO}_3$ . The quartz wool separation technique was repeated at least two more times in order to achieve the maximum possible separation of Pa from Np. The Np/Pa of the spike was assessed after each column by analyzing a dilution with the Nu Plasma MC-ICPMS at

Lawrence Livermore National Laboratory (LLNL). A 5-10  $\mu\text{L}$  aliquot of the spike was diluted  $\sim 1000\times$ , and the solution was screened by measuring the signal intensity of  $^{237}\text{Np}$  and  $^{233}\text{Pa}$  on the ion-counting electron multipliers. Purification of Pa was considered adequate when the signal intensity of  $^{237}\text{Np}$  was an order of magnitude lower than the signal intensity of  $^{233}\text{Pa}$ . Production of  $^{233}\text{Pa}$  from the alpha decay of  $^{237}\text{Np}$  is negligible for  $^{237}\text{Np}/^{233}\text{Pa} < 0.1$ , which represents a Pa/Np separation factor of approximately  $10^{10}$ . At the same time, the amount of  $^{233}\text{Pa}$  available was estimated from the screening dilution and the instrument sensitivity factors, and the final spike solutions were prepared in an appropriate volume of 1 M  $\text{HNO}_3 + 0.05 \text{ M HF}$  so that  $^{233}\text{Pa}$  would be approximately  $1.5 \text{ to } 3 \times 10^{10}$  atoms/g-spike.

Three  $^{233}\text{Pa}$  spikes were prepared for this study (Table 1). Calibration of each  $^{233}\text{Pa}$  spike was performed by isotope dilution mass spectrometry (IDMS) using  $^{231}\text{Pa}$  as the tracer isotope. Because no certified reference material for  $^{231}\text{Pa}$  concentration exists, we used the rock standard Table Mountain Latite (TML), which is generally agreed to have the natural radioactive decay-series in secular equilibrium (Williams *et al.*, 1992) and has been used by the geochemistry community for  $^{233}\text{Pa}$  tracer calibration (e.g. Pickett *et al.*, 1994; Regelous *et al.*, 2004). The concentration of  $^{231}\text{Pa}$  (atoms  $^{231}\text{Pa}$  / g TML) can be calculated by measuring the  $^{235}\text{U}$  concentration by IDMS and using Equation 1,

$$n_{231} = \frac{n_{235}\lambda_{235}}{\lambda_{231}} \quad (\text{Equation 1})$$

where  $n_{235}$  and  $n_{231}$  are atoms of  $^{235}\text{U}$  per gram of TML and atoms of  $^{231}\text{Pa}$  per gram of TML, and  $\lambda_{235}$  and  $\lambda_{231}$  are the decay constants of  $^{235}\text{U}$  and  $^{231}\text{Pa}$ , respectively. However, well-known difficulties involved in the separation of Pa from silicate matrices (*e.g.* Kraus and Moore, 1955; Kim *et al.*, 1973) were observed here as well. After dissolution of TML by standard methods using HF there may be Al- and Na-bearing fluoride compounds in solution that are highly compatible with Pa and notoriously difficult to dissolve. Low Pa recovery was observed in some TML calibration samples. We interpret this as incomplete destruction of such compounds which prevents Pa from behaving predictably in acidic ionic solution. Approximately half of the attempted TML calibration samples failed, and only the results for those analyses with Pa recoveries greater than 10% are listed in Table 1.

Spike calibration was also performed using NBL CRM U100, a nominally 10 % enriched ( $10.190 \pm 0.010$  atom %  $^{235}\text{U}$ ) uranium isotopic reference material with a reported purification date of 8-Jan-1959. Williams and Gaffney (2011) used the  $^{234}\text{U}$ - $^{230}\text{Th}$  chronometer on duplicate solutions of U100 to obtain dates of 16-Feb-1959  $\pm$  88 days and 6-Mar-1959  $\pm$  91 days. Uncertainties on the  $^{234}\text{U}$ - $^{230}\text{Th}$  dates overlap with the reported purification date. These results demonstrate that chemical purification of  $^{234}\text{U}$  from the daughter nuclide  $^{230}\text{Th}$  was complete (negligible initial  $^{230}\text{Th}$  on the date of most recent purification). Until a certified  $^{231}\text{Pa}$  tracer is available, and if the  $^{231}\text{Pa}$  concentration on the purification date is also negligible, U100 is an ideal material to use for  $^{233}\text{Pa}$  tracer calibration, avoiding

the difficulties observed in separating Pa from the silicate matrix of TML. The atomic ratio of  $^{231}\text{Pa}/^{235}\text{U}$  can be calculated for any given time using Equation 2,

$$\frac{n_{231}}{n_{235}} = \frac{\lambda_{235}}{\lambda_{231} - \lambda_{235}} (1 - e^{(\lambda_{235} - \lambda_{231})t}) \quad (\text{Equation 2})$$

where  $n_{231}$  is the number of atoms of  $^{231}\text{Pa}$ ,  $n_{235}$  is the number of atoms of  $^{235}\text{U}$ ,  $t$  is the time from purification,  $\lambda_{235}$  is the decay constant of  $^{235}\text{U}$ , and  $\lambda_{231}$  is the decay constant of  $^{231}\text{Pa}$ . Calibration of the  $^{233}\text{Pa}$  tracer using TML and U100 should produce the same result, if the initial  $^{231}\text{Pa}$  in U100 is negligible. The results presented here indicate that it is negligible, and are addressed in detail below.

To calibrate the  $^{233}\text{Pa}$  tracer, aliquots of TML and U100 containing between  $5 \times 10^8$  and  $1 \times 10^{10}$  atoms of  $^{231}\text{Pa}$  were transferred to Teflon beakers. Approximately the same number of atoms of  $^{233}\text{Pa}$  from the spike was added (typically 0.25-3 g of  $^{233}\text{Pa}$  spike). The mixture was equilibrated by heating, sealed, on a hot plate for several hours. After equilibration,  $\sim 50 \mu\text{L}$  concentrated  $\text{HClO}_4$  was added to each mixture. Chemical separation of Pa was similar to the procedure used for separating Pa from Np, with a few modifications. After the mixtures were dried down, they were re-dissolved in 1 mL 9 M HCl + 50  $\mu\text{L}$  concentrated  $\text{HNO}_3$  + 15  $\mu\text{L}$  saturated  $\text{H}_3\text{BO}_3$ . A  $\sim 2$  mL resin bed of AG-1 X8 (100-200 mesh) was prepared in Poly-Prep columns, and the resin was conditioned with  $>6$  mL 9 M HCl. Samples were loaded on columns, and the vials and columns were washed with 9 M HCl to remove matrix elements while Pa remained sorbed on the resin. New Teflon vials were then placed

underneath the columns, and Pa was eluted using 6 mL of 9 M HCl + 0.05 M HF. A few drops of concentrated HClO<sub>4</sub> were added to each Pa fraction before being dried. Samples were then brought up 1 mL 2 % HNO<sub>3</sub> + 25 μL saturated H<sub>3</sub>BO<sub>3</sub> for Pa separation using the quartz wool technique discussed above. The quartz wool Pa separation was performed twice, with the Pa fractions being dried after the addition of 3-5 drops HClO<sub>4</sub> between. For the second quartz wool step, 3 mL 2 % HNO<sub>3</sub> + 0.005 M HF was used to elute Pa. Samples were not dried down at this point. Instead, this solution was analyzed directly on the day of final separation to minimize in-growth of <sup>233</sup>U from the decay of <sup>233</sup>Pa.

Measurement of <sup>231</sup>Pa/<sup>233</sup>Pa was performed using a Nu Plasma MC-ICP-MS at LLNL. Pa was measured using a static simultaneous pulse-counting routine (40-cycles, 10 second integration time/cycle). Signal intensities on <sup>231</sup>Pa and <sup>233</sup>Pa were typically on the order of 10<sup>3</sup>-10<sup>4</sup> cps for all analyses except low-recovery TML analyses. Masses 235 and 232 were monitored on Faraday detectors to address the completeness of Pa separation from matrix elements (potential tailing of <sup>235</sup>U or <sup>232</sup>Th-hydride at mass 233). The signal intensities of acid blanks, measured before each analysis, were typically <1 cps. Corrections for instrumental mass bias and detector cross-calibration factors were determined by measuring the uranium isotopic standard U010.

The spike concentration (atoms <sup>233</sup>Pa / g-spike) is calculated using Equation 3,

$$n_{233} = \frac{n_{231} \cdot m_{std}}{m_{spike} \cdot R} \quad (\text{Equation 3})$$

where  $n_{233}$  is the number of atoms of  $^{233}\text{Pa}$  per gram of spike,  $n_{231}$  is the calculated number of atoms of  $^{231}\text{Pa}$  per gram of TML solution (Equation 1) or U100 solution (Equation 2),  $R$  is the measured  $^{231}\text{Pa}/^{233}\text{Pa}$  ratio, and  $m_{std}$  and  $m_{spike}$  are the masses (in grams) of the standard solution and spike solution used for the calibration sample, respectively.

The  $^{233}\text{Pa}$  tracer calibration curve is a mathematical model of the decay of  $^{233}\text{Pa}$  over time. The curve is calculated for any time  $t$  (relative to the time of the calibration point analysis) using Equation 4,

$$N_{233t} = N_{233C} e^{(-\lambda_{233}t)} \quad (\text{Equation 4})$$

where  $N_{233t}$  is the number of atoms of  $^{233}\text{Pa}$  per gram of spike at time  $t$ ,  $N_{233C}$  is the measured number of atoms of  $^{233}\text{Pa}$  per gram of spike at the time of calibration (result of Equation 3), and  $\lambda_{233}$  is the decay constant of  $^{233}\text{Pa}$ . Calibration checks are measured throughout the working-life of each spike (about 3-4 months) in order to assess the accuracy of the calibration over time. Calibration curves and calibration points are shown in panels A, C, and E of Figure 1. The uncertainty envelope of each calibration curve, and the position of each calibration point with respect to the calibration curve, is shown in panels B, D, and F of Figure 1.

The  $^{233}\text{Pa}$  tracers, Pa spike-1 and Pa spike-2, were calibrated using both TML and U100 (Figure 1, panels A-D). The Pa spike-1 calibration curve was constructed using TML (calibration point TML-5; Table 1) and the Pa spike-2 calibration curve was constructed using U100 (calibration point U100 #2 (1); Table 1). The accuracy of each curve was assessed throughout the working life of the tracer using replicate measurements of TML and U100. If the assumption of negligible initial  $^{231}\text{Pa}$  underlying Equation 2, and the assumption of secular equilibrium underlying Equation 1, are accurate, then the measured atoms  $^{233}\text{Pa} / \text{g spike}$  for each replicate analysis of TML and U100 should fall within the uncertainty envelope for a given calibration curve, regardless of which standard is used to calibrate the  $^{233}\text{Pa}$  tracer.

The measurement TML (5) was used to construct the Pa spike-1 calibration curve, and the TML (3), U100 #2 (1), and U100 #2 (2) measurements were used as calibration checks (Figure 1, panels A-B). Excellent agreement between TML and U100 is observed for two of the three calibration points: TML (3) and U100 #2 (1) fall within the uncertainty envelope of the calibration curve. Note that U100 #2 (2) falls slightly outside of the uncertainty envelope of the Pa spike-1 calibration curve. This analysis was performed towards the end of the working life of the spike (~4 months after manufacture), and much of the  $^{233}\text{Pa}$  had decayed away at that point. It is also possible that evaporation of the spike over time may have contributed to the slightly higher  $^{233}\text{Pa}$  concentration as determined by U100 #2 (2).

The measurement U100 #2 (1) was used to construct the Pa spike-2 calibration curve, and three TML calibration points and four additional U100 calibration points were used as calibration checks (Figure 1, Panels C-D). Points U100 #2 (2) and U100 #2 (3) were analyzed in the same analytical run as U100 #2 (1); these three points show excellent agreement. U100 #2 (4) and U100 #2 (5) were analyzed approximately 1 and 2 months after calibration, respectively. These two calibration points also fall within the uncertainty envelope of the calibration curve. Poor recovery of Pa from the TML silicate matrix during chemical separation may explain the slight deviation of TML (4) and TML (6) from the calibration curve. TML (5) shows excellent agreement with the U100 calibration curve.

Having established that TML and U100 calibrations produce similar calibration curves, Pa spike-3 was calibrated using only replicate measurements of U100. The measurement of U100 #2 (1) was used to construct the calibration curve, and three replicate measurements of U100 were used as calibration checks. Excellent agreement between all calibration points is observed, even for analyses performed 3-4 months after tracer manufacture.

#### *Isotope dilution measurement of uranium reference standards*

Concentrations of  $^{235}\text{U}$  and  $^{231}\text{Pa}$  were measured by IDMS in uranium reference standards U005-A, U030, U100, U630, and CRM 125-A. In the case of U100, a separate digestion of the starting material (U100 #1) was used. Solutions U005-A,

U030, and U100 were the same solutions analyzed using the  $^{234}\text{U}$ - $^{230}\text{Th}$  chronometer by Williams and Gaffney (2011). Two new digestions each of U630 and CRM 125-A were prepared. The  $^{234}\text{U}$ - $^{230}\text{Th}$  ages of these materials were determined and are reported here for the first time. Measurements of  $^{235}\text{U}$  concentration were made by IDMS with a  $^{233}\text{U}$  spike following the analytical routines described by Williams and Gaffney (2011). Analyses were performed on a Nu Plasma MC-ICPMS using a static routine with  $^{235}\text{U}$  and  $^{233}\text{U}$  measured on Faraday detectors. Correction for instrumental mass bias was made using the uranium isotopic standard U010.

$^{231}\text{Pa}$  was measured by IDMS in these samples using the procedures and  $^{233}\text{Pa}$  spikes described above. The sample concentration of  $^{231}\text{Pa}$  is calculated for the time of analysis using Equation 5,

$$n_{231} = \frac{R \cdot m_{spike} \cdot n_{233}^0 \cdot e^{(-\lambda_{233}t)}}{m_{sample}} \quad (\text{Equation 5})$$

where  $n_{231}$  is the number of atoms of  $^{231}\text{Pa}$  per gram of sample,  $R$  is the  $^{231}\text{Pa}/^{233}\text{Pa}$  measured ratio,  $m_{spike}$  is the spike mass in grams,  $n_{233}^0$  is the number of atoms of  $^{233}\text{Pa}$  per gram of spike on the date of calibration,  $\lambda_{233}$  is the decay constant of  $^{233}\text{Pa}$ ,  $t$  is the number of days between initial spike calibration and analysis, and  $m_{sample}$  is the sample mass in grams. Procedural blanks were also prepared and measured with each analysis batch using the same spiking and chemical separation

procedures as for the samples. Signal intensities for the blanks at  $^{231}\text{Pa}$  were negligible at  $<1$  cps, and no procedural blank corrections were made.

Ages are calculated using Equation 6,

$$t = \left( \frac{1}{\lambda_{235} - \lambda_{231}} \right) \ln \left( 1 + \frac{R(\lambda_{235} - \lambda_{231})}{\lambda_{235}} \right) \quad (\text{Equation 6})$$

where  $t$  is the  $^{235}\text{U}$ - $^{231}\text{Pa}$  age,  $\lambda_{235}$  is the decay constant of  $^{235}\text{U}$ ,  $\lambda_{231}$  is the decay constant of  $^{231}\text{Pa}$ , and  $R$  is the  $^{231}\text{Pa}/^{235}\text{U}$  ratio. All uncertainty calculations in this study follow the guidelines of JCGM 100:2008. An uncertainty budget for the  $^{235}\text{U}$ - $^{231}\text{Pa}$  age of U100 #1 is presented in Table 2. The sources of uncertainty in the  $^{235}\text{U}$ - $^{231}\text{Pa}$  age, in order of decreasing importance, are:

- 1)  $^{231}\text{Pa}/^{233}\text{Pa}$  measurement of the sample;
- 2)  $^{231}\text{Pa}/^{233}\text{Pa}$  measurement for spike calibration;
- 3) the decay constant of  $^{235}\text{U}$  in the calculation of atoms  $^{231}\text{Pa}$  / g U100 standard for the spike calibration (Equation 2);
- 4) isotope dilution measurement of atoms of  $^{235}\text{U}$  / g sample;
- 5) the decay constant of  $^{235}\text{U}$  in the calculation of the age (Equation 6), and
- 6) the decay constant of  $^{233}\text{Pa}$  used in the calculation of sample  $^{231}\text{Pa}$  concentration (Equation 5).

The uncertainties from weighing and the decay constant of  $^{231}\text{Pa}$  contribute  $<0.01$  %. As the largest component of the uncertainty on the age is related to the measurement of  $^{231}\text{Pa}/^{233}\text{Pa}$ , efforts to improve this technique should focus on this. However, the low concentration of  $^{231}\text{Pa}$  in uranium-rich materials produced in the

Nuclear Age presents an intrinsic challenge. In addition, efforts to improve ratio measurements would do nothing to improve upon the inherent uncertainty posed by the initial presence of  $^{231}\text{Pa}$  in the case of incompletely purified samples.

## RESULTS

Ages for U100 (solution #1) and four additional NBL CRMs are presented in Table 3. Measurement of U100 #1 resulted in a  $^{235}\text{U}$ - $^{231}\text{Pa}$  date of 2-Oct-1958  $\pm$  321 days. This date overlaps within uncertainty of the  $^{234}\text{U}$ - $^{230}\text{Th}$  date of 16-Feb-1959  $\pm$  88 days, measured on the same solution by Williams and Gaffney (2011). That both systems are also in agreement with the purification date of 8-Jan-1959 adds confidence in the accuracy of these analyses, and that the assumptions intrinsic to the dating hold true for this sample.

Solutions of U005-A and U030-A were also the same as those analyzed by Williams and Gaffney (2011). Two solutions of each standard were measured (#1 and #2; Table 3), and the two solutions of U005-A were each measured in duplicate. The average  $^{235}\text{U}$ - $^{231}\text{Pa}$  dates of four U005-A analyses and two U030-A analyses are 26-Apr-1980 and 19-Apr-1980, respectively (results for individual analyses are presented in Table 3 and Figure 2).  $^{235}\text{U}$ - $^{231}\text{Pa}$  dates for these standards overlap within uncertainty with the  $^{234}\text{U}$ - $^{230}\text{Th}$  dates of Williams and Gaffney (2011). However, both sets of dates are older than the reported purification dates. These

results suggest that initial  $^{230}\text{Th}$  and  $^{231}\text{Pa}$  concentrations are non-negligible in these standards, resulting in older ages.

The  $^{235}\text{U}$ - $^{231}\text{Pa}$  and  $^{234}\text{U}$ - $^{230}\text{Th}$  dates of U630 and CRM 125-A are presented in Table 3 and Figure 2. These standards do not have reported purification dates and are currently in the process of being certified for  $^{234}\text{U}$ - $^{230}\text{Th}$  age by New Brunswick Laboratory. Average model dates of three U630 analyses (on solutions #1 and #2) and four CRM 125-A (solutions #1 and #2) analyses are 28-Sep-1989 and 16-May-1994, respectively, overlapping within uncertainty with those determined for this study using the  $^{234}\text{U}$ - $^{230}\text{Th}$  chronometer (27-Nov-1988 and 25-Jan-1994, respectively). In this case, the concordant dates indicate that the most recent chemical purification reduced Th and Pa to the same degree with respect to U. The assumption of age-dating, that both were reduced to zero at this time, cannot be proved.

In a nuclear forensic investigation, confidence that ages record the most recent chemical purification event is increased when more than one chronometer is used. The  $^{235}\text{U}$ - $^{231}\text{Pa}$  chronometer can be used in concert with the more frequently-utilized  $^{234}\text{U}$ - $^{230}\text{Th}$  chronometer to assess age accuracy. Ages were concordant for both chronometers for all of the NBL CRMs measured in this study, but are not necessarily consistent with the known purification dates. These results suggest that the  $^{230}\text{Th}/^{234}\text{U}$  and  $^{231}\text{Pa}/^{235}\text{U}$  at the time of uranium purification were small but similar.

Auspices statement, LLNL-release number, funding acknowledgment?

Prepared by LLNL under Contract DE-AC52-07NA27344

## REFERENCES

Cheng H; Edwards RL; Murrell MT; Benjamin TM. 1998. Uranium-thorium-protactinium dating systematics. *Geochimica et Cosmochimica Acta* 62, 3437-3452.

Jones RT; Merritt JS; Okazaki A. 1986. A measurement of the thermal neutron capture cross section of  $^{232}\text{Th}$ . *Nuclear Science and Engineering* 93, 171-180.

Kim JI; Lagally H; Born H-J. 1973. Ion exchange in aqueous and in aqueous-organic solvents. Part I. Anion-exchange behavior of Zr, Nb, Ta and Pa in aqueous HCl-HF and in HCl-HF- organic solvent. *Analytica Chimica Acta* 64, 29-43.

Kraus KA; Moore GE. 1955. Anion-exchange studies. XV. Separation of protactinium and iron by anion-exchange in HCl-HF solutions. *Journal of the American Chemical Society* 77, 1383-1384.

LaMont SP; Hall G. 2005. Uranium age determination by measuring the  $^{230}\text{Th}/^{234}\text{U}$  ratio. *Journal of Radioanalytical and Nuclear Chemistry* 264, 423-427.

Moody KJ; Hutcheon ID; Grant PM. 2005. *Nuclear Forensic Analysis*. CRC Press, Boca Raton, FL, XX p.

Morgenstern A; Apostolidis C; Mayer K. 2002. Age determination of highly enriched uranium: separation and analysis of  $^{231}\text{Pa}$ . *Analytical Chemistry* 74, 5513-5516.

Pickett DA; Murrell MT; Williams RW. 1994. Determination of femtogram quantities of protactinium in geologic samples by thermal ionization mass spectrometry. *Analytical Chemistry* 66, 1044-1049.

Regelous M; Turner SP; Elliott TR; Rostami K; Hawkesworth CJ. 2004. Measurement of femtogram quantities of protactinium in silicate rock samples by multicollector inductively coupled plasma mass spectrometry. *Analytical Chemistry* 76, 3584-3589.

Sims, K.W.W., *et al.* 2008. An Inter-Laboratory Assessment of the Thorium Isotopic Composition of Synthetic and Rock Reference Materials. *Geostandards and Geoanalytical Research*, 32 (1), 65-91.

Varga Z; Nicholl A; Wallenius M; Mayer K. 2012. Development and validation of a methodology for uranium radiochronometry reference material preparation. *Analytica Chimica Acta* 718, 25-31.

Varga Z; Surányi G. 2007. Production date determination of uranium-oxide materials by inductively coupled plasma mass spectrometry. *Analytica Chimica Acta* 599, 16-23.

Varga Z; Wallenius M; Mayer K; Hrncsek E. 2011. Alternative method for the production date determination of impure uranium ore concentrate samples. *Journal of Radioanalytical and Nuclear Chemistry* 290, 485-492.

Williams RW; Collerson KD; Gill JB; Deniel C. 1992. High Th/U ratios in subcontinental lithospheric mantle: mass spectrometric measurement of Th isotopes in Gaussberg lamproites. *Earth and Planetary Science Letters* 111, 257-268.

Williams RW; Gaffney AM. 2011.  $^{230}\text{Th}$ - $^{234}\text{U}$  model ages of some uranium standard reference materials. *Radiochimica Acta* 1, 31-35.

Xiaolong H; Ping L; Wang B. 2005. Evaluation of  $^{233}\text{Pa}$  decay data. *Applied Radiation and Isotopes* 62, 797-804.

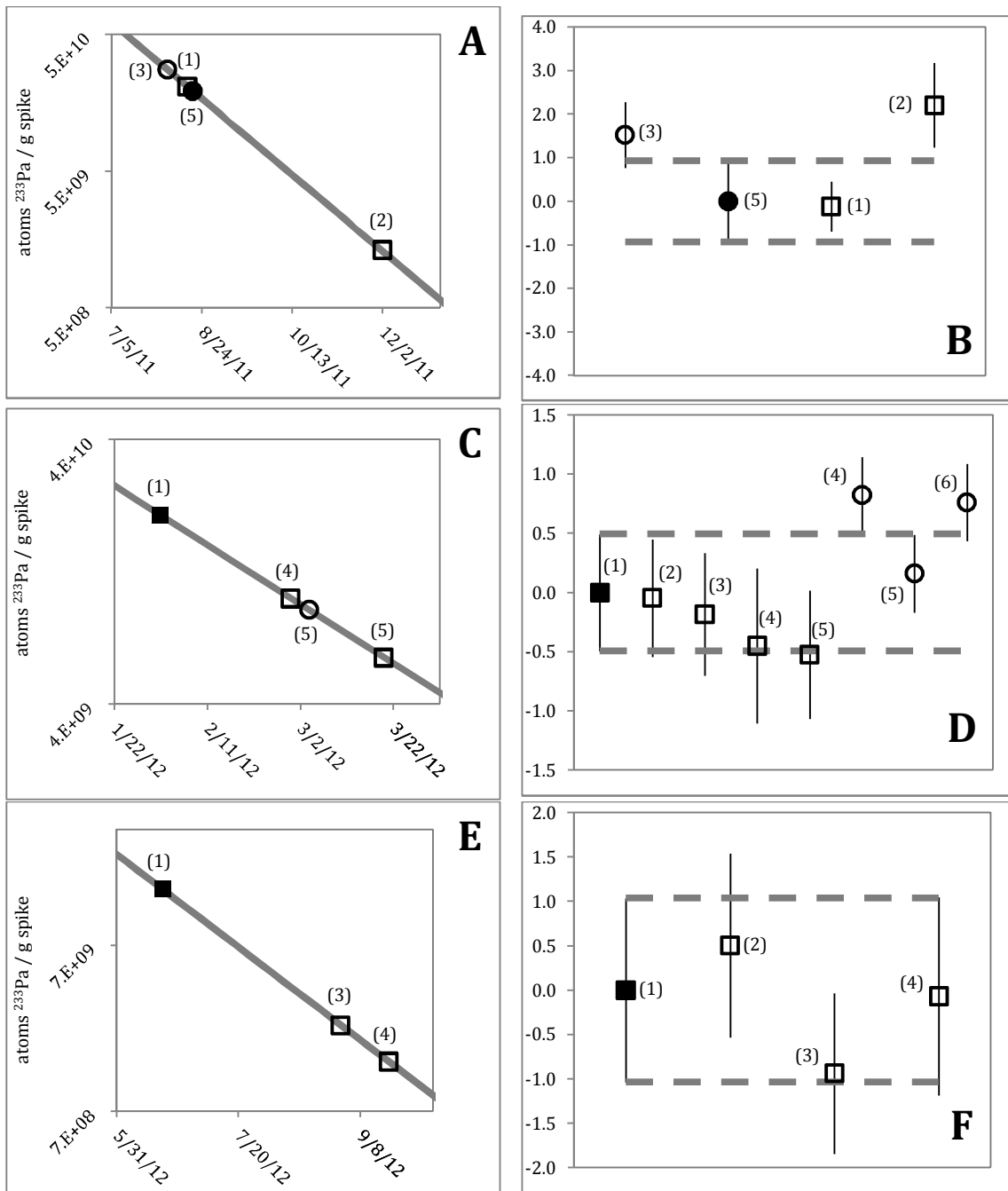


Figure 1. Calibration curves and calibration points for Pa spike-1 (panels A-B), Pa spike-2 (panels C-D), and Pa spike-3 (panels E-F). See Table 1 for calibration point data. Squares, U100 calibration points; circles, TML calibration points; data labels, analysis identification number (see Table 1). In panels A, C, and E, the solid gray line is the calibration curve (calculated using Equation 4), which represents the decay of  $^{233}\text{Pa}$  in each spike over time. The y-axis scales in panels A, C, and E are logarithmic. Closed symbols represent the calibration point upon which the calibration curve is built. In panels B, D, and F, the dotted gray lines represent the uncertainty envelope of the calibration curve. The y-axis scales of panels B, D, and F represent the % difference from the number of atoms of  $^{233}\text{Pa}$  / g spike as defined by the black calibration points. Uncertainty bars in panels A, C, and E are smaller than the symbols.

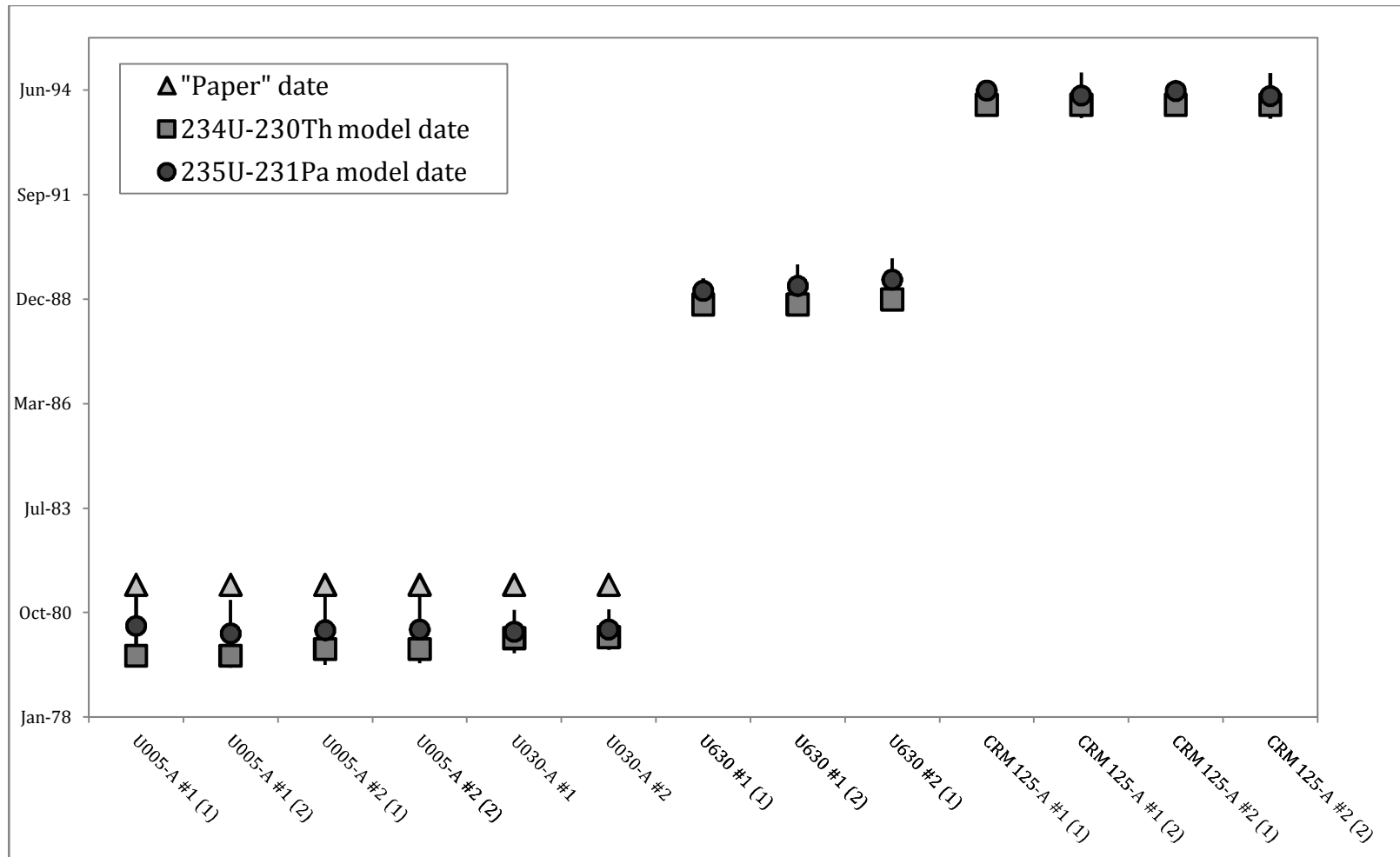


Figure 2. Model ages of uranium standard reference materials.  $^{234}\text{U}$ - $^{230}\text{Th}$  model ages are from Williams and Gaffney (2011). Uncertainty bars for  $^{234}\text{U}$ - $^{230}\text{Th}$  model ages are smaller than symbols. "Paper" dates are reported without uncertainty.

Table 1.  $^{233}\text{Pa}$  spike calibration data. See supplemental online material for calculation of  $^{233}\text{Pa}/\text{g}$  spike by isotope dilution. Data in bold represent the calibration point used to construct the calibration curve for each spike. Data used to calculate measured atoms  $^{233}\text{Pa}/\text{g}$  spike is explained in the text, using data from Supplementary Table 1 (U100) and Supplementary Table 2 (TML). Calculation of the calibration curve atoms  $^{233}\text{Pa}/\text{g}$  spike is explained in the text, using the decay constant  $\lambda^{233}\text{Pa} = 2.5704\text{E}-2$  (Jones *et al.*, 1986).

Sample	Analysis date/time	Measured atoms $^{233}\text{Pa}$ / g spike	Standard Uncertainty	% uncert.	Calibration curve atoms $^{233}\text{Pa}$ / g spike	Standard Uncertainty	Difference (calibration curve - measured)	% difference
<i>Pa spike-1</i>								
TML (3)	8/4/11 19:26	2.808E+10	2.1E+08	0.76	2.766E+10	2.6E+08	4.200E+08	1.52
<b>TML (5)</b>	<b>8/18/11 18:27</b>	<b>1.932E+10</b>	<b>1.8E+08</b>	<b>0.93</b>	<b>1.932E+10</b>	<b>1.8E+08</b>	-	-
U100 #2 (1)	8/15/11 20:04	2.081E+10	1.2E+08	0.58	2.083E+10	1.9E+08	-2.580E+07	-0.12
U100 #2 (2)	12/1/11 17:44	1.330E+09	1.3E+07	0.97	1.301E+09	1.2E+07	2.870E+07	2.21
<i>Pa spike-2</i>								
<b>U100 #2 (1)</b>	<b>1/31/12 15:40</b>	<b>2.081E+10</b>	<b>1.0E+08</b>	<b>0.49</b>	<b>2.081E+10</b>	<b>1.0E+08</b>	-	-
U100 #2 (2)	1/31/12 16:06	2.079E+10	1.0E+08	0.50	2.080E+10	1.0E+08	-9.481E+06	-0.05
U100 #2 (3)	1/31/12 16:32	2.076E+10	1.1E+08	0.52	2.079E+10	1.0E+08	-3.844E+07	-0.18
U100 #2 (4)	2/28/12 19:16	1.005E+10	6.6E+07	0.65	1.009E+10	5.0E+07	-4.550E+07	-0.45
U100 #2 (5)	3/19/12 18:52	6.008E+09	3.3E+07	0.54	6.040E+09	3.0E+07	-3.172E+07	-0.53
TML (4)	3/3/12 19:09	9.185E+09	2.9E+07	0.32	9.110E+09	4.5E+07	7.496E+07	0.82
TML (5)	3/3/12 19:35	9.120E+09	3.0E+07	0.33	9.105E+09	4.5E+07	1.452E+07	0.16
TML (6)	3/3/12 20:02	9.170E+09	3.0E+07	0.33	9.101E+09	4.5E+07	6.927E+07	0.76
<i>Pa spike-3</i>								
<b>U100 #2 (1)</b>	<b>6/18/12 17:49</b>	<b>1.527E+10</b>	<b>1.6E+08</b>	<b>1.04</b>	<b>1.527E+10</b>	<b>1.6E+08</b>	-	-
U100 #2 (2)	6/18/12 18:15	1.534E+10	1.6E+08	1.04	1.526E+10	1.6E+08	7.659E+07	0.50
U100 #2 (3)	8/30/12 20:03	2.311E+09	2.1E+07	0.91	2.333E+09	2.4E+07	-2.189E+07	-0.94
U100 #2 (4)	9/19/12 15:42	1.401E+09	1.6E+07	1.12	1.402E+09	1.5E+07	-9.733E+05	-0.07

Table 2. Representative uncertainty budget.

U100 #1 Model Age		Contribution to combined uncertainty (%)
model age		
	$\lambda^{235}\text{U}$	0.69
	$\lambda^{231}\text{Pa}$	<0.01
	$^{231}\text{Pa}/^{235}\text{U}$	
	atoms $^{235}\text{U}$ / g sample	1.01
	atoms $^{231}\text{Pa}$ / g sample	
	$^{231}\text{Pa} / ^{233}\text{Pa}$	62.82
	spike weight	<0.01
	sample weight	<0.01
	days since initial $^{233}\text{Pa}$ spike calibration	<0.01
	$\lambda^{233}\text{Pa}$	0.02
	atoms $^{233}\text{Pa}$ / g spike	
	standard aliquot weight	<0.01
	spike weight	<0.01
	$^{231}\text{Pa} / ^{233}\text{Pa}$	30.25
	atoms $^{231}\text{Pa}$ / g standard	
	$\lambda^{235}\text{U}$	5.20
	$\lambda^{231}\text{Pa}$	<0.01
	time	<0.01
Total		100.00

Table 3. Model ages of NBL CRMs.

Sample ID	Reference date	atoms 231Pa / g sample	Standard Uncertainty	atoms 235U / g sample	Standard Uncertainty	231Pa / 235U	Standard Uncertainty	235U-231Pa model age	Expanded uncertainty (years, k = 2)	Model date
U005-A #1 (1)	30-Aug-12	6.596E+08	9.0E+06	2.078E+16	1.7E+13	3.174E-08	4.4E-10	32.243	0.887	3-Jun-80
U005-A #1 (2)	30-Aug-12	6.636E+08	9.1E+06	2.078E+16	1.7E+13	3.194E-08	4.4E-10	32.442	0.889	22-Mar-80
U005-A #2 (1)	30-Aug-12	5.374E+08	7.5E+06	1.687E+16	1.4E+13	3.186E-08	4.4E-10	32.358	0.902	21-Apr-80
U005-A #2 (2)	30-Aug-12	5.371E+08	7.4E+06	1.687E+16	1.4E+13	3.184E-08	4.4E-10	32.338	0.889	29-Apr-80
U030-A #1	28-Feb-12	4.089E+08	3.6E+06	1.303E+16	9.6E+12	3.140E-08	2.8E-10	31.889	0.567	9-Apr-80
U030-A #2	28-Feb-12	2.764E+08	2.3E+06	8.819E+15	6.6E+12	3.134E-08	2.6E-10	31.830	0.530	30-Apr-80
U100 #1	28-Feb-12	1.772E+09	1.4E+07	3.372E+16	2.8E+13	5.257E-08	4.3E-10	53.407	0.879	2-Oct-58
U630 #1 (1)	19-Mar-12	2.142E+09	1.5E+07	9.452E+16	1.4E+14	2.266E-08	1.6E-10	23.018	0.334	13-Mar-89
U630 #1 (2)	29-Jun-12	2.156E+09	2.6E+07	9.452E+16	1.4E+14	2.281E-08	2.8E-10	23.167	0.561	29-Apr-89
U630 #2 (1)	29-Jun-12	2.521E+10	3.0E+08	1.113E+18	1.4E+15	2.265E-08	2.7E-10	23.004	0.554	27-Jun-89
CRM 125-A #1 (1)	19-Mar-12	1.010E+10	7.1E+07	5.772E+17	7.7E+14	1.750E-08	1.3E-10	17.773	0.257	11-Jun-94
CRM 125-A #1 (2)	28-Jun-12	1.033E+10	1.7E+08	5.772E+17	7.7E+14	1.790E-08	2.9E-10	18.175	0.598	26-Apr-94
CRM 125-A #2 (1)	19-Mar-12	1.381E+10	9.7E+07	7.886E+17	1.0E+15	1.751E-08	1.2E-10	17.782	0.255	7-Jun-94
CRM 125-A #2 (2)	28-Jun-12	1.412E+10	2.3E+08	7.886E+17	1.0E+15	1.791E-08	2.9E-10	18.190	0.599	20-Apr-94
Sample ID	Reference date	atoms 230Th / g sample	Standard Uncertainty	atoms 234U / g sample	Standard Uncertainty	230Th / 234U	Standard Uncertainty	234U-230Th model age	Expanded uncertainty (years, k = 2)	Model date
U630 #1 (1)	19-Mar-12	6.098E+10	2.1E+08	9.232E+14	1.5E+12	6.605E-05	2.5E-07	23.372	0.184	3-Nov-88
U630 #1 (2)	19-Mar-12	6.098E+10	2.1E+08	9.232E+14	1.5E+12	6.605E-05	2.5E-07	23.372	0.184	3-Nov-88
U630 #2 (1)	29-May-12	7.201E+11	1.8E+09	1.087E+16	1.6E+13	6.623E-05	1.9E-07	23.434	0.142	21-Dec-88
CRM 125-A #1 (1)	19-Mar-12	2.729E+11	9.4E+08	5.321E+15	4.3E+13	5.129E-05	4.5E-07	18.147	0.321	25-Jan-94
CRM 125-A #1 (2)	19-Mar-12	2.729E+11	9.4E+08	5.321E+15	4.3E+13	5.129E-05	4.5E-07	18.147	0.321	25-Jan-94
CRM 125-A #2 (1)	19-Mar-12	3.728E+11	1.3E+09	7.269E+15	5.9E+13	5.128E-05	4.5E-07	18.146	0.321	25-Jan-94
CRM 125-A #2 (2)	19-Mar-12	3.728E+11	1.3E+09	7.269E+15	5.9E+13	5.128E-05	4.5E-07	18.146	0.321	25-Jan-94

Supplementary Table 1. Data for the calculation of atoms  $^{233}\text{Pa}/\text{g}$  spike by isotope dilution with U100 isotopic standard.  $^{231}\text{Pa}/^{233}\text{Pa}$  was measured on a Nu Plasma MC-ICPMS. Years since production date is the difference between analysis date and the reported U100 production date of 8-Jan-1959. U100  $^{231}\text{Pa}/^{235}\text{U}$  is calculated using  $t$  = years since production date and the following decay constants:  $\lambda^{235}\text{U} = 9.8458\text{E}-10$ ;  $\lambda^{231}\text{Pa} = 2.1133\text{E}-5$ . Atoms of  $^{231}\text{Pa}/\text{g}$  U100 solution is calculated using a measured solution of U100 measured to have a  $^{235}\text{U}$  concentration of  $5.796\text{E}16 \pm 1.024\text{E}14$  atoms/g. Data listed in bold indicates calibration point used to calculate the calibration curve for each spike.

Sample	Analysis date/time	standard mass (g)	Standard Uncertainty	$^{233}\text{Pa}$ spike mass (g)	Standard Uncertainty	$^{231}\text{Pa}/^{233}\text{Pa}$	Standard Uncertainty	years since production date	U100 $^{231}\text{Pa}/^{235}\text{U}$ on analysis date	atoms $^{231}\text{Pa}$ / g U100 sol'n	Standard Uncertainty	atoms $^{233}\text{Pa}$ / g spike	Standard Uncertainty
<i>Pa spike-1</i>													
U100 #2 (1)	8/15/11 20:04	2.2618	0.00019	0.2605	0.00018	1.253	6.8E-03	52.60	5.178E-08	3.001E+09	5.7E+06	2.081E+10	1.2E+08
U100 #2 (2)	12/1/11 17:44	2.3021	0.00018	3.0534	0.00000	1.711	1.6E-02	52.90	5.207E-08	3.018E+09	5.7E+06	1.330E+09	1.3E+07
<i>Pa spike-2</i>													
<b>U100 #2 (1)</b>	<b>1/31/12 15:40</b>	<b>2.3116</b>	<b>0.00008</b>	<b>0.7617</b>	<b>0.00002</b>	<b>0.441</b>	<b>2.0E-03</b>	<b>53.06</b>	<b>5.223E-08</b>	<b>3.027E+09</b>	<b>5.7E+06</b>	<b>2.081E+10</b>	<b>1.0E+08</b>
U100 #2 (2)	1/31/12 16:06	2.3145	0.00004	0.7606	0.00000	0.443	2.0E-03	53.06	5.223E-08	3.027E+09	5.7E+06	2.079E+10	1.0E+08
U100 #2 (3)	1/31/12 16:32	2.3169	0.00007	0.7592	0.00002	0.445	2.1E-03	53.06	5.223E-08	3.027E+09	5.7E+06	2.076E+10	1.1E+08
U100 #2 (4)	2/28/12 19:16	2.3095	0.00004	1.5262	0.00000	0.457	2.9E-03	53.14	5.231E-08	3.032E+09	5.7E+06	1.005E+10	6.6E+07
U100 #2 (5)	3/19/12 18:52	2.3130	0.00002	3.0519	0.00002	0.383	1.9E-03	53.20	5.236E-08	3.035E+09	5.7E+06	6.008E+09	3.3E+07
<i>Pa spike-3</i>													
<b>U100 #2 (1)</b>	<b>6/18/12 17:49</b>	<b>2.2897</b>	<b>0.00003</b>	<b>0.2541</b>	<b>0.00003</b>	<b>1.799</b>	<b>1.8E-02</b>	<b>53.44</b>	<b>5.261E-08</b>	<b>3.049E+09</b>	<b>5.8E+06</b>	<b>1.527E+10</b>	<b>1.6E+08</b>
U100 #2 (2)	6/18/12 18:15	2.2953	0.00006	0.5069	0.00004	0.900	9.2E-03	53.44	5.261E-08	3.049E+09	5.8E+06	1.534E+10	1.6E+08
U100 #2 (3)	8/30/12 20:03	2.2915	0.00003	1.0158	0.00004	2.987	2.6E-02	53.64	5.280E-08	3.060E+09	5.8E+06	2.311E+09	2.1E+07
U100 #2 (4)	9/19/12 15:42	1.7216	0.00002	1.5327	0.00003	2.457	2.7E-02	53.70	5.286E-08	3.064E+09	5.8E+06	1.401E+09	1.6E+07

Supplementary Table 2. Data for the calculation of atoms  $^{233}\text{Pa}/\text{g}$  spike by isotope dilution with Table Mountain Latite (TML), a rock standard in  $^{235}\text{U}/^{231}\text{Pa}$  secular equilibrium (Williams et al., 1992).  $^{231}\text{Pa}/^{233}\text{Pa}$  was measured on a Nu Plasma MC-ICPMS. The measured  $^{235}\text{U}$  concentration of TML is  $7.187\text{E}12 \pm 1.337\text{E}8$  atoms/g. Assuming secular equilibrium, the  $^{231}\text{Pa}$  concentration of TML is  $3.346\text{E}8 \pm 2.824\text{E}5$  atoms/g, calculated using the following decay constants:  $\lambda^{235}\text{U} = 9.8458\text{E}-10$ ;  $\lambda^{231}\text{Pa} = 2.1133\text{E}-5$ . Data listed in bold indicates calibration point used to calculate the calibration curve for that spike.

Sample	Analysis date/time	standard mass (g)	Standard Uncertainty	$^{233}\text{Pa}$ spike mass (g)	Standard Uncertainty	$^{231}\text{Pa}/^{233}\text{Pa}$	Standard Uncertainty	atoms $^{233}\text{Pa}$ / g spike	Standard Uncertainty
<i>Pa spike-1</i>									
TML (3)	8/4/11 19:26	4.1295	0.00005	0.1556	0.00007	0.316	2.4E-03	2.808E+10	2.1E+08
<b>TML (5)</b>	<b>8/18/11 18:27</b>	<b>8.7162</b>	<b>0.00018</b>	<b>0.4630</b>	<b>0.00011</b>	<b>0.326</b>	<b>3.0E-03</b>	<b>1.932E+10</b>	<b>1.8E+08</b>
<i>Pa spike-2</i>									
TML (4)	3/3/12 19:09	2.37100	0.00006	0.5131	0.00006	0.168	5.2E-04	9.185E+09	2.9E+07
TML (5)	3/3/12 19:35	2.34770	0.00006	0.6139	0.00007	0.140	4.5E-04	9.120E+09	3.0E+07
TML (6)	3/3/12 20:02	2.40407	0.00007	0.7152	0.00007	0.123	3.9E-04	9.170E+09	3.0E+07

Supplementary Table 3. Data for isotope dilution calculation of  $^{231}\text{Pa}$  concentration in NBL CRMs. Parenthetical numbers in sample IDs refer to replicate measurements of the same solution of an NBL CRM.  $^{231}\text{Pa}/^{233}\text{Pa}$  was measured on a Nu Plasma MC-ICPMS. Decay-corrected atoms  $^{233}\text{Pa}/\text{g}$  spike is calculated following Equation 3 and using the decay constant  $\lambda_{233} = 2.570\text{E}-2$  (Jones et al., 1986).

Sample	Analysis date/time	233Pa spike	Days from spike calibration date	Decay-corrected atoms 233Pa / g spike	Standard Uncertainty	sample aliquot, g	Standard Uncertainty	233Pa spike aliquot, g	Standard Uncertainty	231Pa / 233Pa	Standard Uncertainty	atoms 231Pa / g sample	Standard Uncertainty
U005-A #1 (1)	8/30/12 17:20	Pa spike-3	72.98	2.339E+09	2.4E+07	9.2121	0.00006	1.0202	0.00008	2.546	2.3E-02	6.596E+08	9.0E+06
U005-A #1 (2)	8/30/12 18:15	Pa spike-3	73.02	2.337E+09	2.4E+07	9.2128	0.00004	1.0197	0.00004	2.566	2.3E-02	6.636E+08	9.1E+06
U005-A #2 (1)	8/30/12 18:42	Pa spike-3	73.04	2.335E+09	2.4E+07	9.2080	0.00006	1.0206	0.00006	2.076	1.9E-02	5.374E+08	7.5E+06
U005-A #2 (2)	8/30/12 19:08	Pa spike-3	73.05	2.334E+09	2.4E+07	9.2160	0.00010	1.0169	0.00010	2.085	1.9E-02	5.371E+08	7.4E+06
U030-A #1	2/28/12 17:57	Pa spike-2	28.10	1.011E+10	1.0E+08	5.8041	0.00003	0.7555	0.00004	0.311	2.3E-03	4.089E+08	3.6E+06
U030-A #2	2/28/12 18:24	Pa spike-2	28.11	1.010E+10	1.0E+08	5.7885	0.00003	0.7612	0.00003	0.208	1.4E-03	2.764E+08	2.3E+06
U100 #1	2/28/12 18:50	Pa spike-2	28.13	1.010E+10	1.0E+08	2.3018	0.00004	0.7577	0.00004	0.533	3.5E-03	1.772E+09	1.4E+07
U630 #1 (1)	3/19/12 16:38	Pa spike-2	48.04	6.053E+09	6.3E+07	7.4722	0.00004	1.0268	0.00002	2.576	1.3E-02	2.142E+09	1.5E+07
U630 #1 (2)	6/29/12 0:22	Pa spike-3	10.27	1.172E+10	1.2E+08	3.1934	0.00004	0.5057	0.00003	1.161	7.1E-03	2.156E+09	2.6E+07
U630 #2 (1)	6/29/12 1:12	Pa spike-3	10.31	1.171E+10	1.2E+08	0.5351	0.00003	0.5063	0.00004	2.275	1.4E-02	2.521E+10	3.0E+08
CRM 125-A #1 (1)	3/19/12 17:30	Pa spike-2	48.08	6.047E+09	6.3E+07	0.5630	0.00005	0.7653	0.00002	1.229	6.2E-03	1.010E+10	7.1E+07
CRM 125-A #1 (2)	6/28/12 15:00	Pa spike-3	9.88	1.184E+10	1.2E+08	0.5581	0.00003	0.5078	0.00003	0.959	1.2E-02	1.033E+10	1.7E+08
CRM 125-A #2 (1)	3/19/12 18:26	Pa spike-2	48.12	6.041E+09	6.2E+07	0.5642	0.00005	0.7651	0.00004	1.686	8.5E-03	1.381E+10	9.7E+07
CRM 125-A #2 (2)	6/28/12 15:00	Pa spike-3	9.88	1.184E+10	1.2E+08	0.5604	0.00003	0.5076	0.00003	1.317	1.7E-02	1.412E+10	2.3E+08